Note: This copy is for your personal non-commercial use only. To order presentation-ready copies for distribution to your colleagues or clients, contact us at www.rsna.org/rsnarights.

Arterial Spin-Label Imaging in Patients with Normal Bolus Perfusion-weighted MR Imaging Findings: Pilot Identification of the Borderzone Sign[1]

Greg Zaharchuk, PhD, MD
Roland Bammer, PhD
Matus Straka, PhD
Ajit Shankaranarayan, PhD
David C. Alsop, PhD
Nancy J. Fischbein, MD
Scott W. Atlas, MD
Michael E. Moseley, PhD

Purpose: To determine whether perfusion abnormalities are depicted on arterial spin-labeling (ASL) images obtained in patients with normal bolus perfusion-weighted (PW) magnetic resonance (MR) imaging findings.

Materials and Methods: Institutional review board approval and written informed patient consent were obtained. This study was HIPAA compliant. Consecutive patients suspected or known to have cerebrovascular disease underwent 1.5-T brain MR imaging, including MR angiography, gradient-echo PW imaging, and pseudocontinuous ASL imaging, between October 2007 and January 2008. Patients with normal bolus PW imaging findings were retrospectively identified, and two neuroradiologists subsequently evaluated the ASL images for focal abnormalities. The severity of the borderzone sign—that is, bilateral ASL signal dropout with surrounding cortical areas of hyperintensity in the middle cerebral artery borderzone regions—was classified by using a four-point scale. For each group, the ASL-measured mean mixed cortical cerebral blood flow (CBF) at the level of the centrum semiovale was evaluated by using the Jonckheere-Terpstra test.

Results: One hundred thirty-nine patients met the study inclusion criteria, and 41 (30%) of them had normal bolus PW imaging findings. Twenty-three (56%) of these 41 patients also had normal ASL imaging findings. The remaining 18 (44%) patients had the ASL borderzone sign; these patients were older (mean age, 71 years ± 11 [standard deviation] vs 57 years ± 16; $P < .005$) and had lower mean CBF (30 mL/100 g/min ± 12 vs 46 mL/100 g/min ± 12, $P < .003$) compared with the patients who had normal ASL imaging findings. Five patients had additional focal ASL findings that were related to either slow blood flow in a vascular structure or postsurgical perfusion defects and were not visible on the PW images.

Conclusion: Approximately half of the patients with normal bolus PW imaging findings had abnormal ASL findings—most commonly the borderzone sign. Results of this pilot study suggest that ASL imaging in patients who have this sign and are suspected of having cerebrovascular disease yields additional and complementary hemodynamic information.

© RSNA, 2009

Supplemental material: *http://radiology.rsnajnls.org/cgi/content/full/2523082018/DC1*

[1] From the Department of Radiology, Stanford University Medical Center, 1201 Welch Rd, PS-04, MC 5488, Stanford, CA 94305-5488 (G.Z., R.B., M.S., N.J.F., S.W.A., M.E.M.); Applied Sciences Laboratory-West, GE Medical Systems, Menlo Park, Calif (A.S.); and Department of Radiology, Beth Israel Deaconess Medical Center, Boston, Mass (D.C.A.). Received November 14, 2008; revision requested January 13, 2009; revision received January 27; accepted March 6; final version accepted March 24. **Address correspondence to** G.Z. (e-mail: *gregz@stanford.edu*).

© RSNA, 2009

Dynamic susceptibility contrast perfusion-weighted (PW) magnetic resonance (MR) imaging has been extensively used clinically to evaluate the hemodynamic abnormalities associated with a wide range of cerebrovascular and cerebral neoplastic diseases (1,2). Analysis of the nondiffusible intravascularly confined contrast material bolus as it passes through the brain capillary bed can yield maps of important hemodynamic parameters, such as cerebral blood flow (CBF), cerebral blood volume, mean transit time, and normalized time to the peak of the residue function. Although several groups have developed methods to determine the absolute values of these parameters (3–6), such quantitation remains challenging (7,8). The bolus PW imaging hemodynamic maps acquired in the majority of patients are evaluated qualitatively by means of comparison of the abnormal and contralateral (presumed normal) regions.

Arterial spin labeling (ASL) enables one to measure CBF without exogenous contrast agents by using a diffusible tracer: magnetically labeled water (9,10). ASL imaging may be particularly useful in children, in those without peripheral intravenous access, and in those with reduced creatinine clearance who are at risk for nephrogenic systemic fibrosis. Owing to technical issues and a relatively low signal-to-noise ratio, ASL has only recently been applied in the clinical setting (11–24). The ability to quantify CBF with use of ASL suggests that this technique could be used to detect bilateral disease, which is often present in patients with cerebrovascular disease (25). Also, ASL is sensitive to prolonged arterial tracer arrival times because the label decays with the longitudinal relaxation rate of the blood. This sensitivity may enable the differentiation between patients who have truly normal cerebral hemodynamic parameters and those who have mild alterations in CBF and arterial arrival time (13). The purpose of this study was to determine whether perfusion abnormalities are depicted on the ASL images obtained in patients with normal bolus PW imaging findings.

Advances in Knowledge

- Abnormalities are often depicted on the arterial spin-labeling (ASL) images obtained in patients with normal bolus perfusion-weighted (PW) imaging findings.
- A bilateral hypoperfusion pattern, which we have termed the *borderzone sign,* was among the most common of these abnormalities.
- In a small subset of patients, focal ASL findings other than the borderzone sign that were related to slow or stagnant arterial flow were seen that were not visible on the PW images.

Materials and Methods

Industrial Support

One of the authors (A.S.), a full-time employee of GE Medical Systems (Menlo Park, Calif), provided the ASL pulse sequence used in this study. The remaining authors, who are not employees of GE Medical Systems, had control of the inclusion of any data and information that might have represented a conflict of interest for the author who is an employee. Another author (D.C.A.) is an inventor of patents related to the ASL techniques described in this article.

Patient Population

All MR examinations were performed as part of the patients' routine clinical care. All patients had signed informed consent forms approved by the institutional review board of Stanford University Medical Center for the prospective study of the safety and utility of advanced imaging sequences between October 2007 and January 2008. This study was Health Insurance Portability and Accountability Act compliant. The study cohort was retrospectively identified (G.Z.) on the basis of the following criteria: The patient was clinically known or suspected to have cerebrovascular disease (as gleaned from the electronic medical record) and had undergone bolus PW imaging and ASL pulse imaging.

Implications for Patient Care

- ASL can help in identifying perfusion alterations in patients with normal bolus PW imaging findings.
- ASL imaging and bolus PW imaging generate different information, and performing both examinations could be considered for patients with cerebrovascular disease to obtain a more complete picture of the brain hemodynamics.

Imaging Methods

The patients were examined with brain MR imaging at 1.5 T (Signa; GE Medical Systems, Milwaukee, Wis). All patients underwent standard intracranial three-dimensional time-of-flight MR angiography with the following parameters: 34/3.1 (repetition time msec/echo time msec), a 24-cm field of view, a matrix of 512 × 128, and 1-mm-thick sections spaced 0.5 mm apart. A superior saturation band was used. All patients also underwent the following nonperfusion-related imaging examinations: axial diffusion-weighted (6000/70, b = 1000 sec/mm^2, three directions), axial gradient-echo (600/30), T2-weighted fast spin-echo (4717/85), and axial fluid-attenuated inversion-recovery (repetition time msec/echo time msec/inversion time msec, 8802/110/2200) imaging. All of these examinations were performed with a 5-mm section thickness and 1.5-mm skip.

For bolus PW imaging, gradient-echo

Published online before print
10.1148/radiol.2523082018

Radiology 2009; 252:797–807

Abbreviations:
ASL = arterial spin labeling
CBF = cerebral blood flow
MCA = middle cerebral artery
PW = perfusion weighted

Author contributions:
Guarantors of integrity of entire study, G.Z., A.S., M.E.M.; study concepts/study design or data acquisition or data analysis/interpretation, all authors; manuscript drafting or manuscript revision for important intellectual content, all authors; manuscript final version approval, all authors; literature research, G.Z., R.B., M.S., M.E.M.; clinical studies, G.Z., R.B., A.S., N.J.F., S.W.A., M.E.M.; statistical analysis, G.Z., M.S.; and manuscript editing, G.Z., M.S., D.C.A., N.J.F., M.E.M.

See Materials and Methods for pertinent disclosures.

echo-planar imaging was performed during the passage of 0.1 mmol of gadopentetate dimeglumine (Magnevist; Berlex Laboratories, Wayne, NJ) or gadodiamide (Omniscan; GE Healthcare, Waukesha, Wis) per kilogram of body weight, which was administered at a rate of 4 mL/sec by using a power injector. Image readout was performed by using standard single-shot echo-planar imaging (2000/60) or multishot multiecho generalized autocalibrating partially parallel acquisition echo-planar imaging (1225/17, 30, 52; acceleration factor of three) (26). Fifteen axial 5-mm-thick sections separated by a 1.5-mm intersection gap encompassed the entire supratentorial region of the brain. The in-plane spatial resolution was 2.6 mm. Acquisition of the bolus PW images required 2 minutes. The raw images were postprocessed by means of automated arterial input function detection and deconvolution with circular singular value decomposition (27). These images yielded the following parameter maps: relative cerebral blood volume, relative CBF, mean transit time, and normalized time to the peak of the residue function.

Pseudocontinuous ASL was performed by using a labeling period of 1500 msec followed by a postlabeling delay of 1500 msec (28). The technical details of this acquisition and postprocessing protocol are discussed in Appendix E1 *(http://radiology.rsnajnls.org/cgi/content/full/2523082018/DC1)* (28,29). Quantitative mixed cortical CBF was measured on a single section at the level of the centrum semiovale by using 10 cortical regions of interest, as shown in Figure 1.

Some, but not all, of the patients were also examined with extracranial vascular imaging—primarily two-dimensional time-of-flight or three-dimensional contrast-enhanced MR angiography. Several patients also underwent computed tomographic (CT) angiography, ultrasonography (US), or conventional (catheter) angiography. Hemodynamically significant stenosis was defined as greater than or equal to 70% luminal narrowing on the basis of North American Symptomatic Carotid Endarterectomy Trial criteria.

Radiologic Assessment

All assessments of the normality of the bolus PW images were based on imaging features, without regard to clinical information. Routine anatomic images that were acquired as part of the patient's clinical protocol were not evaluated in this study. The following method was used to identify normal bolus PW imaging cases: First, any case in which the bolus PW imaging results were explicitly described as abnormal in the final radiology report on the basis of findings on any of the hemodynamic maps (CBF, cerebral blood volume, mean transit time, or normalized time to the peak of the residue function) was excluded. Then, to determine whether any subtle abnormalities that were not apparent at initial radiologic image review were present, a neuroradiologist with 10 years experience examining bolus PW imaging studies (G.Z.) further examined all remaining cases in which the bolus PW imaging examination results were either described as normal at the final radiologic image reading or were not commented on. Again, if an abnormality could be discerned on any hemodynamic map, the patient was excluded.

We found, on the basis of pilot study data, that many ASL images showed low ASL signal, with surrounding cortical areas of high signal intensity in the middle cerebral artery (MCA)-anterior cerebral artery borderzone and MCA–posterior cerebral artery borderzone, a finding that we have termed the *borderzone sign*. For this study, the ASL images were reviewed by two neuroradiologists (S.W.A., N.J.F., both with more than 20 years experience in neuroradiology) with extensive experience interpreting clinical ASL imaging studies. They reviewed the ASL images in a random blinded fashion at separate times by using the same monitor. To assess the severity of the borderzone sign, we created a nominal four-point scale: A score of 0 meant

Figure 1

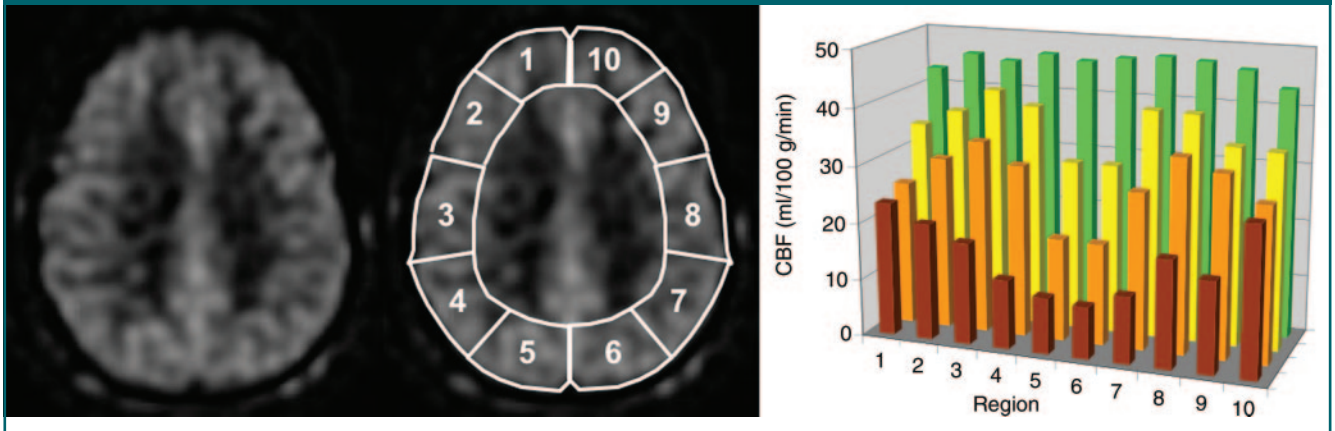

Figure 1: Axial ASL CBF MR images (left) and graph (right) illustrate CBF measurements in 10 cortical regions of interest (regions *1–10*) at level of centrum semiovale. On the graph, red bars indicate ASL score of 3 (three patients); orange bars, score of 2 (five patients); yellow bars, score of 1 (10 patients); and green bars, score of 0 (23 patients). Note the stepwise CBF decrease with increasing ASL score and the regional distribution of measurements, which shows that CBF is most affected in posterior regions (regions *5* and *6*). The population averaged generalized estimating equations regression of CBF on ASL score, region, and their interaction revealed an overall significant negative effect of ASL score ($P < .001$); significant main effects of regions *4* ($P < .035$), *7* ($P < .001$), and *8* ($P < .030$); and significant interactions between ASL score and regions *3* ($P < .003$), *5* ($P < .001$), *6* ($P < .001$), *7* ($P < .038$), and *10* ($P < .001$).

normal findings; 1, a mild borderzone sign; 2, a moderate borderzone sign; and 3, a severe borderzone sign. The reviewers were presented with the ASL images shown in Figure 2 as a template to aid in the scoring. In addition, if the reviewer thought the borderzone sign was present (score of 1, 2, or 3), he or she further categorized it as symmetric or asymmetric. Disagreements were resolved by consensus.

Statistical Analyses

κ Statistics and Spearman rank correlation coefficients (ρ) were used to examine the agreement between the two readers. A two-tailed *t* test was used to compare age between the patients with normal ASL findings and the patients with abnormal ASL findings. Mean differences in CBF between these groups were analyzed by using the Jonckheere-Terpstra test for ordered alter-

Figure 2

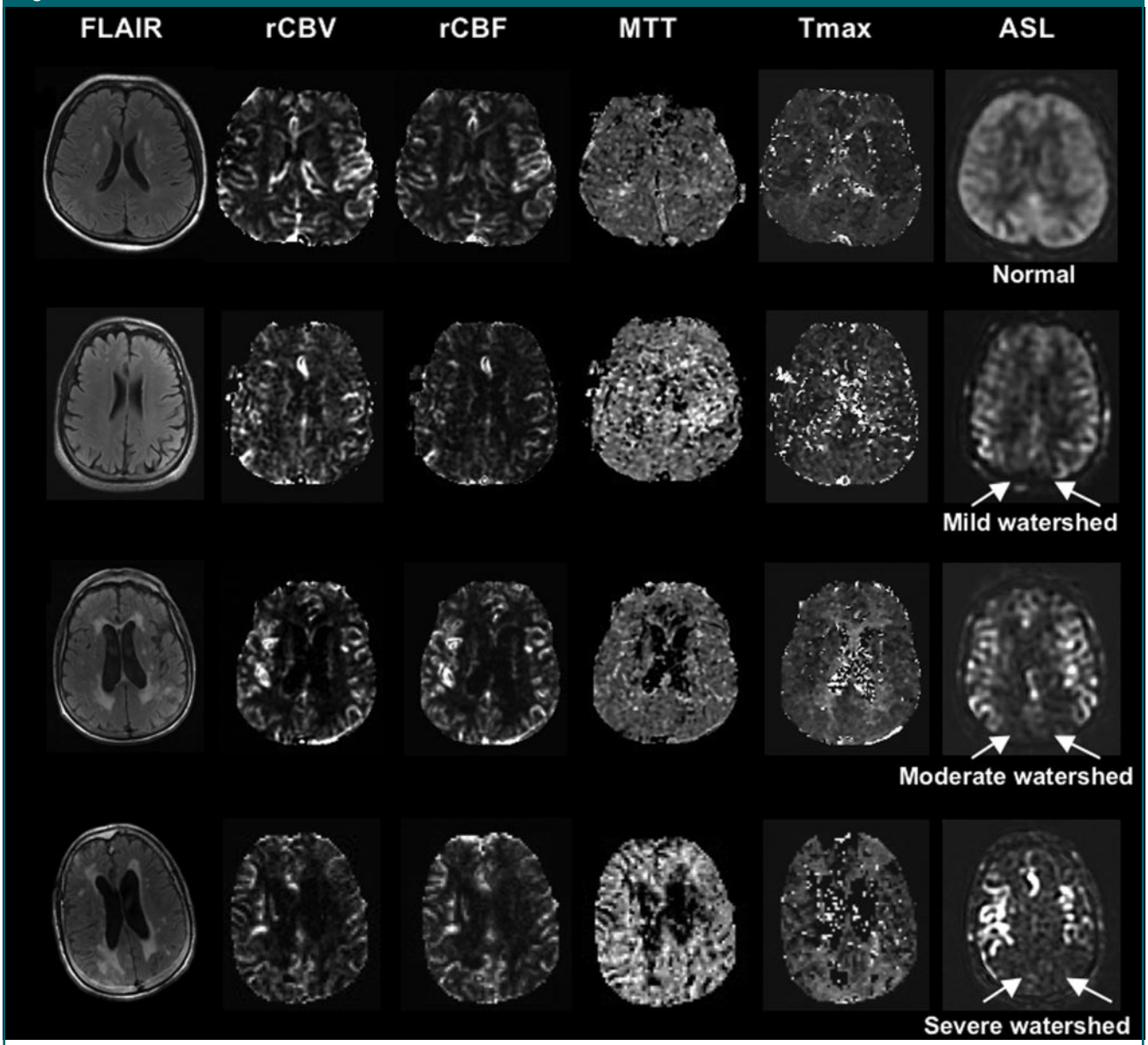

Figure 2: Common ASL imaging findings in four patients (four rows) with normal bolus PW imaging findings. Fluid-attenuated inversion-recovery *(FLAIR)* (8802/110/2200) relative cerebral blood volume *(rCBV),* relative CBF *(rCBF),* mean transit time *(MTT),* and normalized time to peak of the residue function *(Tmax)* maps (1225/17, 30, 52) are shown for comparison. Many ASL images show the borderzone sign (ie, watershed, arrows)—that is, signal dropout in the bilateral MCA–anterior cerebral artery and MCA–posterior cerebral artery borderzones, with serpiginous high signal intensity in the surrounding cortex. The severity of this sign ranges from mild to severe. In the severe case, only the proximal segments of the MCA and anterior cerebral artery are visualized, with a complete absence of parenchymal ASL signal.

natives, which is a parametric test for trends that does not require the use of normally distributed values. CBF differences were analyzed within the different regions and groups by using a population averaged generalized estimating equations (PA-GEE) regression of CBF on ASL score, region, and their interaction. $P < .05$ was considered to indicate a significant difference. All statistical analyses were performed by using Stata, release 9.2, software (Stata, College Station, Tex).

Results

One hundred thirty-nine patients met the criteria for inclusion in the study. In 105 (76%) of these patients, image readout was performed by using parallel multiecho echo-planar MR imaging; the 34 remaining patients underwent single-shot echo-planar PW imaging. Forty-one (30%) (15 men, 26 women; mean age, 63 years ± 15 [standard deviation]) of the 139 patients had normal bolus PW imaging findings. In the majority ($n = 37$, 90%) of these 41 patients, image readout was performed by using parallel multiecho echo-planar imaging. Single-shot echo-planar imaging was used to perform image readout in the four remaining patients.

The clinical indications for the 41 patients included in this study are listed in Table 1. The primary indications were focal weakness and altered mental status. Four patients had symptoms that raised concern about possible transient ischemic attack but were asymptomatic at the time of imaging. Only one patient had a lesion at intracranial MR angiography: a thrombus in a second branch of the MCA, near the MCA bifurcation. Extracranial vascular imaging was performed in 27 (66%) of the 41 patients: MR angiography in nine patients, CT angiography in 14 patients, US in one patient, and conventional angiography in three patients. Two patients had unilateral internal carotid artery occlusion; there were no other hemodynamically significant extracranial lesions. Patient demographic data are presented in Table 2.

Lesions indicating acute ischemic stroke were seen on the diffusion-weighted images obtained in 13 (32%) of the 41 patients; most of these lesions were small. The following lesions were seen: four pure borderzone infarcts, which were bilateral in two patients; one small insular infarct with associated ipsilateral borderzone infarct; one cerebellar hemisphere infarct with associated bilateral borderzone infarcts; three lacunae in the deep gray nuclei; one infarct in the caudate head-body region; one infarct in the splenium of the corpus callosum; one small cortical infarct in the anterior cerebral artery territory; and one pontine infarct. In seven (54%) of these 13 patients, at least a component of the diffusion-weighted imaging lesion was in the borderzone region. The diffusion-weighted imaging findings, with associated demographics and ASL scores, are presented in Tables 2 and 3.

Results of the reviewers' evaluation of the ASL abnormalities are shown in Table 4. The Kendall τ_b score and the nonweighted κ value for the concordance between the two reviewers were 0.62 ($P < .001$) and 0.32 ($P < .001$), respectively. The reviewers differed by two scale points in their scores for only two (5%) of the 41 patients. Their agreement in assigning normal versus abnormal ratings was even higher ($\kappa = 0.56$, $P < .001$). Results of the consensus reading are shown in Figure 3. Twenty-three (56%) of the 41 patients had normal findings at ASL imaging—namely, homogeneous, symmetric parenchymal CBF signal intensity (Fig 2, top row). In the remaining 18 patients, ASL signal loss was seen in the bilateral MCA–anterior cerebral artery and MCA–posterior cerebral artery borderzone regions, with serpiginous high signal intensity in the surrounding cortex, forming the borderzone sign. The severity of this sign ranged from mild to severe (Fig 2, second to fourth rows). In the severe cases, only the major second branches of the middle cerebral and anterior cerebral arteries were visualized, with absent parenchymal signal.

The patients with normal ASL imaging findings were younger than those with the borderzone sign (57 years ± 16 [standard deviation] vs 71 years ± 11, $P < .005$). The ASL scores assigned to the 27 patients who underwent extracranial vascular imaging and the 25 patients proved not to have hemodynamically significant stenosis in the intra- or extracranial vascular circulation ($n = 25$) are presented in Table 3.

There was reduced concordance between the two reviewers in determining whether the borderzone sign, if present, was symmetric ($\kappa = 0.13$, $P > .05$). In nine (50%) of 18 cases, the reviewers agreed: in five cases of a symmetric borderzone sign and four cases of an asymmetric sign. In eight (89%) of the nine remaining cases, the same reviewer identified asymmetry while the other reviewer saw a symmetric appearance, reflecting the reviewers' different sensitivities. The final consensus determination was that 12 (67%) of the 18 patients had a symmetric borderzone sign.

The mean mixed cortical CBF at the level of the centrum semiovale was decreased in the patients with the borderzone sign compared with that in the patients with normal ASL findings (30 mL/100 g/min ± 12 vs 46 mL/100 g/min ± 12, $P < .003$). Also, there was a stepwise decrease in CBF with increasing ASL score ($P < .001$, Table 5). The data in Figure 1 show that the CBF decreases were primarily in the posterior borderzone regions.

Additional focal abnormalities were seen on the ASL images obtained in five (12%) patients: Two patients had linear high ASL signal near small diffusion lesions (Fig 4). Two other patients had high ASL signal that rep-

Table 1

Primary Clinical Indications in Study Patients

Indication	No. of Patients
Focal weakness	15
Altered mental status	11
Sensory abnormality*	5
Generalized weakness	2
Vertigo	2
Headache	2
Aphasia	1
Neoplasm	1
Subarachnoid hemorrhage	1
Seizure	1
Total	41

* Numbness and/or tingling.

resented slow or stagnant flow in a vascular structure: in a cavernous carotid artery aneurysm in one patient and in the cavernous carotid stump ipsilateral to an internal carotid artery occlusion in the other (Fig 5). The remaining patient had low ASL signal in postsurgical resection cavities in the cerebellum and left frontal lobe of the brain (Fig 6).

Discussion

Results of this study show that additional information is available on ASL images obtained in patients with normal bolus PW imaging findings. Approximately half of the cases were also normal at ASL imaging, and the normal cases occurred in younger patients. In most of the remaining cases, we detected what we have termed the *borderzone sign*—that is, bilateral dropout of ASL signal in the MCA–anterior cerebral artery and MCA–posterior cerebral artery vascular borderzones, with serpiginous high signal intensity in the surrounding cortex. We believe that the serpiginous high signal intensity represents labeled blood remaining in feeding arteries that has yet to reach the capillary beds, a finding that has been termed *arterial transit artifact* by prior researchers (13,17).

Most of the time, the borderzone sign was symmetric, although cases of asymmetry were also seen. MCA borderzones have long arterial tracer arrival times (29), and we believe that the borderzone sign is a reflection of longer-than-normal arrival times, slower CBF, or a combination of these phenomena. Reduced CBF may be the most common since CBF and arterial arrival times are often affected together, as in cases of

Table 2

Patient Demographic Information

Characteristic	All Patients	Male Patients	Female Patients	Patients with Abnormal ASL Findings	Patients with Normal ASL Findings
No. of patients	41	15	26	18	23
Mean patient age (y)*	63 (21–89)	66 (21–89)	62 (34–84)	71 (51–89)	57 (21–84)
Intracranial MR angiography performed	41 (100)	15 (100)	26 (100)	18 (100)	23 (100)
Hemodynamically significant intracranial lesion†	1 (2)	1 (7)	0	1 (6)	0
Extracranial vascular imaging performed	27 (66)	10 (67)	17 (65)	14 (78)	13 (57)
Hemodynamically significant extracranial lesion‡	2 (7)	2 (20)	0	1 (7)	1 (8)
DW imaging high signal intensity	13 (32)	9 (60)	4 (15)	8 (44)	5 (22)

Note.—All except age data are numbers of patients. Unless otherwise noted, numbers in parentheses are percentages based on data in No. of patients row. DW = diffusion weighted.

* Numbers in parentheses are age ranges.

† Hemodynamically significant (≥70% luminal narrowing, according to North American Symptomatic Carotid Endarterectomy Trial criteria) lesion seen at intracranial MR angiography. The lesion in the patient with abnormal ASL findings was a filling defect in the second branch of the MCA, near the MCA bifurcation.

‡ Hemodynamically significant lesion seen at extracranial vascular imaging. The percentages of patients with these lesions are based on the numbers of patients who underwent extracranial vascular imaging (in directly preceding row). Both the lesion in the patient with abnormal ASL findings and the lesion in the patient with normal ASL findings were unilateral internal carotid artery occlusions.

Table 3

ASL Scores Based on Vascular Imaging Status

Characteristic	Total*	ASL Score†				Lesion Seen at DW Imaging†
		0	1	2	3	
All patients	41	23 (56)	10 (24)	5 (12)	3 (7)	13 (32)
Extracranial vascular imaging performed	27 (66)	13 (48)	9 (33)	4 (15)	1 (4)	11 (41)
Extracranial vascular imaging not performed	14 (34)	10 (71)	1 (7)	1 (7)	0 (0)	2 (14)
No significant stenosis or occlusion in head or neck‡	25 (61)	12 (48)	9 (36)	3 (12)	1 (6)	10 (40)
Documented significant stenosis or occlusion in head or neck‡	2 (7)§	1 (50)	0 (0)	1 (50)	0 (0)	1 (50)

Note.—Data are numbers of patients, all of whom underwent intracranial nonenhanced three-dimensional time-of-flight MR angiography. An ASL score of 0 indicated normal ASL imaging findings; 1, mild borderzone sign; 2, moderate borderzone sign; and 3, severe borderzone sign. DW = diffusion weighted.

* Unless otherwise noted, numbers in parentheses are percentages based on total of 41 patients.

† Numbers in parentheses are percentages based on numbers of patients in Total column.

‡ Significant stenosis was defined as greater than or equal to 70% luminal narrowing according to North American Symptomatic Carotid Endarterectomy Trial criteria.

§ Both lesions were unilateral internal carotid occlusions, one of which also showed evidence of thrombus near the contralateral MCA bifurcation at intracranial MR angiography. Percentage is based on number of patients examined with extracranial vascular imaging ($n = 27$).

acute ischemic stroke (30). Possible causes might include underlying small-vessel disease, reduced cardiac output, and true underlying reduced CBF. In theory, bolus PW imaging parameters such as normalized time to the peak of the residue function are sensitive to arterial arrival delays—albeit only to those delays greater than or equal to the repetition time in the bolus PW imaging sequence. However, review of the data for even those patients with a severe ASL borderzone sign did not reveal marked differences from the other patients in this study. This finding suggests that there is a possible synergistic interaction between longer arrival times and truly reduced CBF on ASL images. Delineating the specific effects of arrival time and CBF on the appearance of the borderzone sign requires the use of ASL sequences that are sensitive to different arrival times, such as those involving acquisitions at multiple postlabeling delay times (31,32).

With stroke and other low-blood-flow diseases, CBF quantification is confounded by the ASL signal loss related to the delayed arterial arrival time (33). For this reason, we focused our current study on the qualitative clinical evaluation of ASL images. However, we did observe that the measured CBF (with the effects of arterial arrival time ignored) decreased with increasing ASL score, demonstrating that the ASL score, while arbitrarily defined, does appear to correlate with a measure of perfusion. Longer postlabeling delay times can be used to improve CBF quantitation, but at the expense of low signal-to-noise ratios on perfusion images. Alternatively, ASL images can be obtained with multiple postlabeling delay times and then fitted for both CBF and arterial arrival time. However, these acquisitions are performed at the expense of a low signal-to-noise ratio or an increased imaging time (29) and are prone to the instability of nonlinear curve-fitting algorithms. In the current study, we used a postlabeling delay of 1500 msec, which in prior reports has been suggested to be too short for quantitative CBF measurements in elderly patients (34). However, such timing might be beneficial in that it would enable the sensitive detection of subtle perfusion alterations, even when the CBF remained normal (35).

The presence and frequency of the borderzone sign probably depend on the pulse sequence parameters—particularly the labeling time and the postlabeling delay—and whether vessel-suppression tools such as small diffusion gradients (36,37) are used. It is unclear whether the vascular signal should be suppressed at routine brain imaging. Vascular signal suppression decreases the conspicuity of slow-blood-flow regions and vascular malformations (16), but it enables more straightforward image interpretation in the setting of reperfusion or neoplasm.

In a minority of cases, additional focal findings that were not seen on the bolus PW images were identified on the ASL images. These findings might have been attributed to fewer and less severe susceptibility artifacts, a lack of parenchymal signal contamination by large-vessel artifact, and the sensitivity of ASL to slow-flowing arterial blood. The spatial resolution and signal-to-noise ratio of bolus PW images are limited by the need to image

Table 4

Distribution of ASL Scores Assigned by the Two Reviewers

Reviewer 1 Score	Reviewer 2 Score 0	1	2	3	Total
0	14*	5	0	0	19
1	3	4*	2	1	10
2	1	4	1*	1	7
3	0	0	2	3*	5
Total	18	13	5	5	41

Note.—Data are numbers of patients with the given ASL scores. An ASL score of 0 indicated normal ASL imaging findings; 1, mild borderzone sign; 2, moderate borderzone sign; and 3, severe borderzone sign. Reviewers were presented with the ASL images in Figure 2 as a template to grade normal ASL findings versus mild, moderate, and severe borderzone signs.

* Agreement between the two reviewers regarding the ASL score (Kendall $\tau_b = 0.62$, $P < .001$; Spearman $\rho = 0.69$, $P < .0001$; nonweighted $\kappa = 0.32$, $P < .001$; linearly weighted $\kappa = 0.54$, $P < .001$).

Figure 3

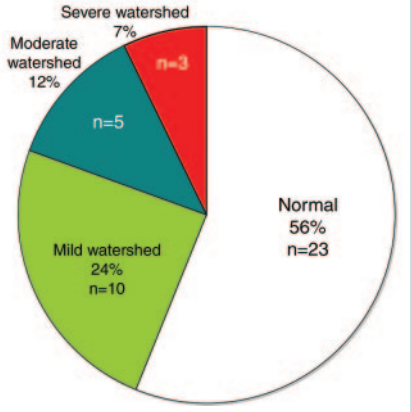

Figure 3: Pie chart shows distribution of borderzone sign (ie, watershed) severity in patients with normal PW imaging findings at consensus reading. Nearly half of the patients had abnormal ASL findings, with varying degrees (mild to severe) of the borderzone sign.

Table 5

Mean CBF Values in Patients with Different ASL Findings

Patient Group	ASL Score	CBF (mL/100 g/min)
Patients with normal ASL findings	0	45.8 ± 11.8
Patients with mild borderzone sign	1	36.0 ± 9.4*
Patients with moderate borderzone sign	2	27.6 ± 9.2*
Patients with severe borderzone sign	3	16.6 ± 9.9*
Patients with any degree of borderzone sign	1, 2, or 3	30.4 ± 11.5†
All patients	0–3	39.1 ± 13.9

Note.—All CBF measurements are means ± standard deviations.

* Significant decrease in CBF with increasing ASL score ($P < .001$).

† Significant CBF decrease between patients with normal ASL findings (score of 0) and patients with abnormal ASL findings (score of 1, 2, or 3) ($P < .003$).

rapidly to sample the contrast material bolus; fast imaging methods such as single-shot echo-planar imaging yield susceptibility artifacts in regions such as the posterior fossa and the inferior frontal and inferior temporal lobes. Some of these drawbacks can be addressed by using parallel techniques (26).

ASL is not bound by the requirement to image fast, although most prior implementations of this technique have involved the use of echo-planar imaging because of errors introduced by patient motion. Background suppression makes ASL images less sensitive to motion, so other readout methods can be used (38–40). In the current study, we used three-dimensional fast spin-echo readout, which is among the approaches that are the most insensitive to susceptibility artifacts. This was demonstrated by our ability to visualize structures in the posterior fossa and near postsurgical resection cavities (Fig 6). Use of three-dimensional readout also improves the signal-to-noise ratio and permits straightforward reformatting of the data in arbitrary imaging planes, which is important for coregistering the data with those in prior imaging studies.

Finally, ASL imaging tends to be less sensitive to large vessels because it involves the use of a diffusible tracer (water) that exchanges freely with brain parenchymal water. In the current study, signal remaining in the arterial vessels was identified, but this reflected an underlying physiologic abnormality. Two patients with reduced diffusion due to small acute ischemic infarcts had intraarterial ASL signal (Fig 4), which may have represented stagnant flow upstream of an arterial occlusion or even late-arriving collateral flow (13,17). Chalela et al (13) reported this ASL finding in seven of 15 patients with acute ischemic stroke, and it appeared to represent tissue that did not become infarcted. We also observed high ASL signal indicative of stagnant or slow flow in patients with known vascular abnormalities: in an aneurysm in one patient and in the stump of a proximally occluded cavernous carotid artery in another patient. The described ASL method cannot compare with MR angiography in the depiction of these kinds of lesions, but it may have added diagnostic value in patients in whom such findings are not expected and thus MR angiography is not routinely performed. Abnormal pooling of ASL signal in a characteristic location near the circle of Willis could then prompt dedicated angiographic imaging.

This small study had several limitations. There was no control subject population, such as that of patients imaged for indications other than suspected or known cerebrovascular disease. Therefore, we cannot theorize as to the frequency of the borderzone sign in other patient populations. In addition, we examined only those patients with normal bolus PW imaging findings and thus excluded any potential cases in which the abnormalities seen on PW images might

Figure 4

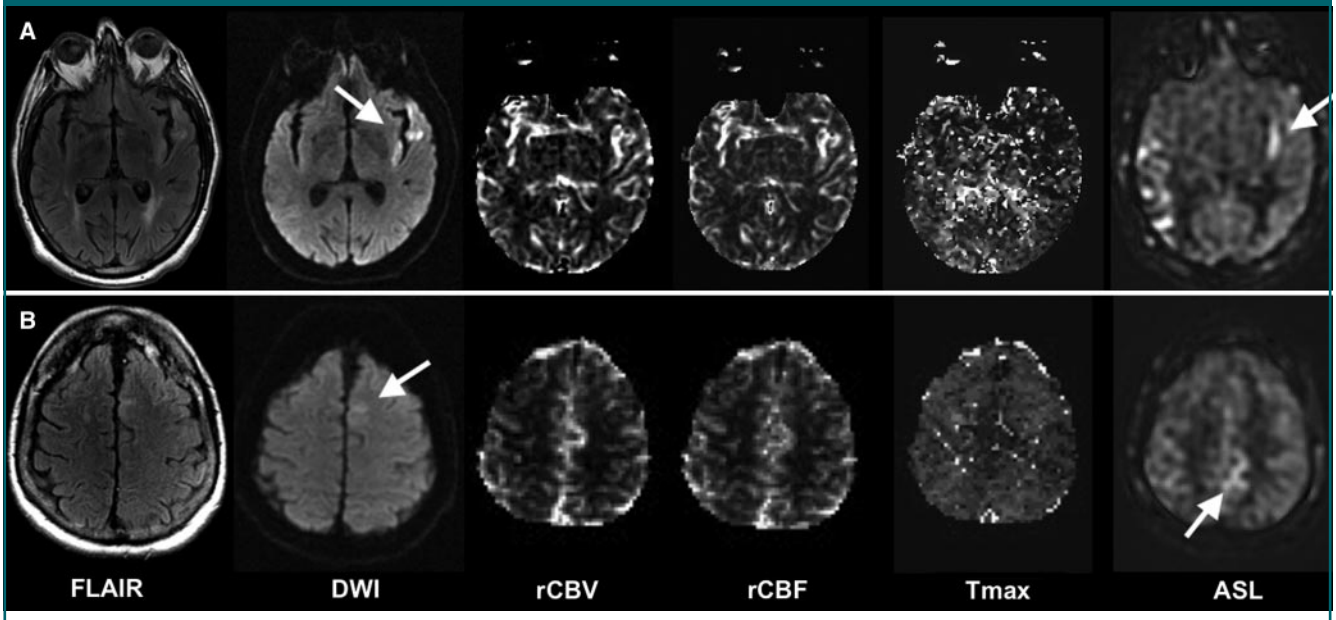

Figure 4: Fluid-attenuated inversion-recovery *(FLAIR)* (8802/110/2200), diffusion-weighted *(DWI)* (6000/70, $b = 1000$ sec/mm^2), and ASL images, and relative cerebral blood volume *(rCBV)*, relative CBF *(rCBF)*, and normalized time to peak of the residue function *(Tmax)* maps (1225/17, 30, 52) obtained in two patients with linear high ASL signal near brain regions with reduced diffusion. Both patients had normal bolus PW imaging findings. *A*, Imaging findings in 76-year-old man 3 days after acute onset of aphasia, right-side weakness, and visual disturbance. Diffusion-weighted image shows positive lesions (arrow) in and around left insula. ASL image shows linear increased signal intensity (arrow) in left insula; this lesion possibly represents slow blood flow or recanalization. *B*, Imaging findings in 77-year-old woman with difficulty rising from a chair. On diffusion-weighted image, the region of focal diffusion abnormality (arrow) in left anterior cerebral artery territory is subtle but was thought to represent early infarction. On ASL image, the linear high signal (arrow) in area immediately posterior to diffusion abnormality may represent slow antegrade arterial or collateral blood flow.

not be seen on ASL images. Also, there is no reference standard for the borderzone sign; it cannot be observed on PW images on the basis of the inclusion criteria used for this study. The stepwise decrease in apparent CBF with increasing ASL score, however, suggests that there is an underlying quantitative difference that this scale is capturing. The CBF decrease with increasing ASL score may be partially explained by the reviewers' use of low ASL signal as a grading criterion, although this was only one of the criteria used for ASL scoring. Cortical high signal intensity was the other criterion. Also, it should be noted that PW imaging methods involving shorter repetition times should be capable of revealing more subtle alterations in both normalized time to the peak of the residue function and mean transit time. The majority (90%) of the patients in this study were examined with a parallel PW imaging sequence involving a very short repetition time (1225 milliseconds), although several patients underwent conventional PW imaging involving a repetition time of 2000 milliseconds.

Given these limitations, this study should be regarded as a pilot investigation to identify a potentially interesting radiologic finding that could be more rigorously examined in future studies. It would be particularly interesting to prospectively follow-up patients who have the borderzone sign to determine the clinical importance of this finding. Possible studies could include the follow-up of such patients to determine if they are at higher risk for subsequent stroke, whether the borderzone sign correlates with disease in other organ systems, and/or whether the sign is associated with specific physiologic conditions such as hypertension. Also, we recognize that the CBF values that we report may be erroneously low owing to prolonged arterial arrival times, which were not measured in this study, especially in those patients with high ASL scores. However, our goal in including this information was to show that the objective perfusion measurements followed the expected pattern with the ASL scores rather than to serve as a reference standard. Finally, we wish to emphasize that the goal of this study was not to determine which perfusion measurement method was better; rather, it was to demonstrate the relationships between the methods and show that the different sensitivities to tracer arrival time may enable the visualization of ab-

Figure 5

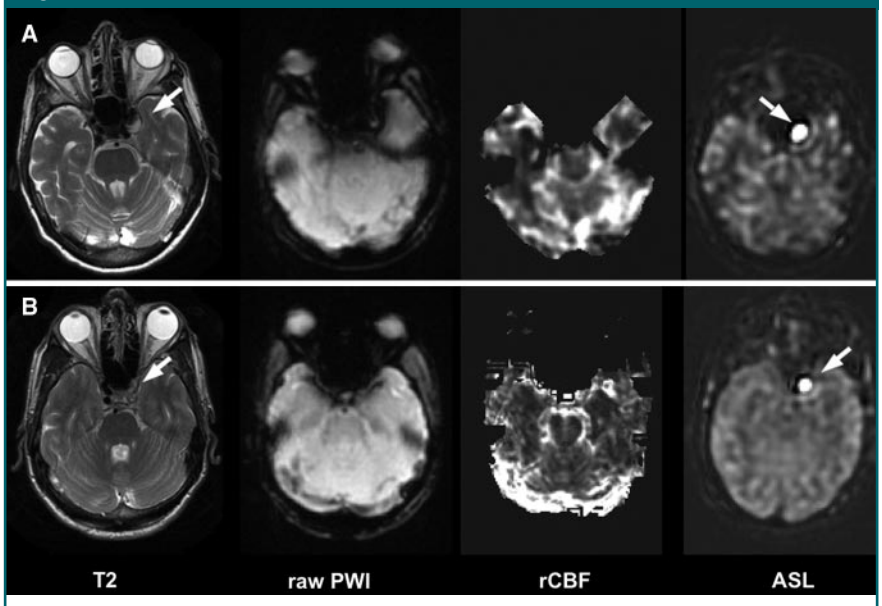

Figure 5: High ASL signal in setting of stagnant or slow blood flow in vascular structures. T2-weighted fast spin-echo *(T2)* (4717/85), raw gradient-echo echo-planar PW *(PWI)* (1225/17), and ASL MR images, and relative CBF *(rCBF)* maps (1225/17, 30, 52) are shown for comparative purposes. *A,* Imaging findings in 84-year-old woman with a 15-mm left cavernous carotid aneurysm (arrows). *B,* Imaging findings in 58-year-old man with chronic left internal carotid artery occlusion (arrow on T2-weighted image) at carotid bifurcation. On ASL image, the high signal (arrow) in ipsilateral cavernous carotid artery possibly represents slow or stagnant retrograde blood flow via the anterior communicating and/or ophthalmic arteries.

Figure 6

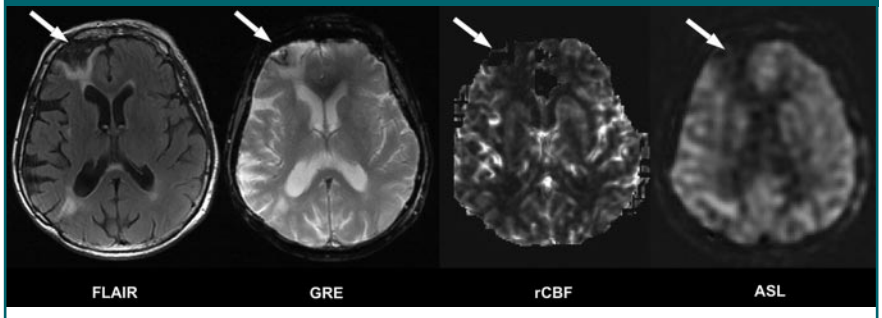

Figure 6: Low ASL signal in right frontal resection cavity in 78-year-old woman with history of surgery for meningioma removal, who presented with right lower-extremity weakness and numbness after a mechanical fall. Fluid-attenuated inversion-recovery *(FLAIR)* (8802/110/2200), gradient-echo *(GRE)* (600/30), and ASL MR images, and relative CBF *(rCBF)* map (1225/17, 30, 52) obtained at bolus PW imaging are shown for comparison. Although the lesion (arrows) is clearly evident on the images obtained with anatomic sequences, the ASL image shows a lack of blood flow in the cavity and normal perfusion to the surrounding tissue. This region is poorly visualized on the relative CBF map obtained at bolus PW imaging, possibly owing to susceptibility artifacts caused by the hemosiderin lining the resection cavity.

normalities on ASL images obtained in patients with normal bolus PW imaging findings.

In conclusion, ASL imaging revealed additional abnormalities in about half of the patients with normal bolus PW imaging findings. The most common abnormality was the borderzone sign—that is, bilateral ASL signal loss in the MCA–anterior cerebral artery and MCA–posterior cerebral artery borderzones. This finding is associated with increased age, and we believe it is related to a combination of increased arterial arrival time and reduced CBF. In a minority of cases, other findings that also might be useful in the clinical diagnosis and management were seen. Thus, performing ASL imaging as an additional examination may be considered in cases of suspected or known cerebrovascular disease.

References

1. Sorensen AG, Buonanno FS, Gonzalez RG, et al. Hyperacute stroke: evaluation with combined multisection diffusion-weighted and hemodynamically weighted echo-planar MR imaging. Radiology 1996;199(2):391–401.
2. Cha S, Knopp E, Johnson G, Wetzel S, Litt A, Zagzag D. Intracranial mass lesions: dynamic contrast-enhanced susceptibility-weighted echo-planar perfusion MR imaging. Radiology 2002;223(1):11–29.
3. Ostergaard L, Weisskoff RM, Chesler DA, Gyldensted C, Rosen BR. High resolution measurement of cerebral blood flow using intravascular tracer passages. I. Mathematical approach and statistical analysis. Magn Reson Med 1996;36(5):715–725.
4. Lin W, Celik A, Derdeyn C, et al. Quantitative measurements of cerebral blood flow in patients with unilateral carotid artery occlusion: a PET and MR study. J Magn Reson Imaging 2001;14(6):659–667.
5. Carroll TJ, Teneggi V, Jobin M, et al. Absolute quantification of cerebral blood flow with magnetic resonance, reproducibility of the method, and comparison with H2(15)O positron emission tomography. J Cereb Blood Flow Metab 2002;22(9):1149–1156.
6. Takasawa M, Jones PS, Guadagno JV, et al. How reliable is perfusion MR in acute stroke? validation and determination of the penumbra threshold against quantitative PET. Stroke 2008;39(3):870–877. [Published correction appears in Stroke 2008; 39(8):e141.]
7. van Osch MJ, van der Grond J, Bakker CJ. Partial volume effects on arterial input functions: shape and amplitude distortions and their correction. J Magn Reson Imaging 2005;22(6):704–709.
8. Jochimsen TH, Newbould RD, Skare ST, et al. Identifying systematic errors in quantitative dynamic-susceptibility contrast perfusion imaging by high-resolution multi-echo parallel EPI. NMR Biomed 2007;20(4):429–438.
9. Dixon WT, Du LN, Faul DD, Gado M, Rossnick S. Projection angiograms of blood labeled by adiabatic fast passage. Magn Reson Med 1986;3(3):454–462.
10. Detre JA, Leigh JS, Williams DS, Koretsky AP. Perfusion imaging. Magn Reson Med 1992;23(1):37–45.
11. Detre JA, Samuels OB, Alsop DC, Gonzalez-At JB, Kasner SE, Raps EC. Noninvasive magnetic resonance imaging evaluation of cerebral blood flow with acetazolamide challenge in patients with cerebrovascular stenosis. J Magn Reson Imaging 1999;10(5):870–875.
12. Detre JA, Alsop DC. Perfusion magnetic resonance imaging with continuous arterial spin labeling: methods and clinical applications in the central nervous system. Eur J Radiol 1999;30(2):115–124.
13. Chalela JA, Alsop DC, Gonzalez-Atavales JB, Maldjian JA, Kasner SE, Detre JA. Magnetic resonance perfusion imaging in acute ischemic stroke using continuous arterial spin labeling. Stroke 2000;31(3):680–687.
14. Silva AC, Kim SG, Garwood M. Imaging blood flow in brain tumors using arterial spin labeling. Magn Reson Med 2000;44(2):169–173.
15. Weber MA, Thilmann C, Lichy MP, et al. Assessment of irradiated brain metastases by means of arterial spin-labeling and dynamic susceptibility-weighted contrast-enhanced perfusion MRI: initial results. Invest Radiol 2004;39(5):277–287.
16. Wolf RL, Wang J, Detre JA, Zager EL, Hurst RW. Arteriovenous shunt visualization in arteriovenous malformations with arterial spin-labeling MR imaging. AJNR Am J Neuroradiol 2008;29(4):681–687.
17. Wolf RL, Alsop DC, McGarvey ML, Maldjian JA, Wang J, Detre JA. Susceptibility contrast and arterial spin label perfusion MRI in cerebrovascular disease. J Neuroimaging 2003;13(1):17–27.
18. Wolf RL, Wang J, Wang S, et al. Grading of CNS neoplasms using continuous arterial spin labeled perfusion MR imaging at 3 Tesla. J Magn Reson Imaging 2005;22(4): 475–482.
19. Weber MA, Gunther M, Lichy MP, et al. Comparison of arterial spin-labeling techniques and dynamic susceptibility-weighted contrast-enhanced MRI in perfusion imaging of normal brain tissue. Invest Radiol 2003; 38(11):712–718.
20. Pollock JM, Whitlow CT, Deibler AR, et al. Anoxic injury-associated cerebral hyperperfusion identified with arterial spin-labeled MR imaging. AJNR Am J Neuroradiol 2008; 29(7):1302–1307.
21. Deibler AR, Pollock JM, Kraft RA, Tan H, Burdette JH, Maldjian JA. Arterial spin-labeling in routine clinical practice. I. Technique and artifacts. AJNR Am J Neuroradiol 2008;29(7):1228–1234.
22. Deibler AR, Pollock JM, Kraft RA, Tan H, Burdette JH, Maldjian JA. Arterial spin-labeling in routine clinical practice. II. Hypoperfusion patterns. AJNR Am J Neuroradiol 2008;29(7):1235–1241.
23. Deibler AR, Pollock JM, Kraft RA, Tan H, Burdette JH, Maldjian JA. Arterial spin-labeling in routine clinical practice. III. Hyperperfusion patterns. AJNR Am J Neuroradiol 2008;29(8):1428–1435.
24. Pollock JM, Deibler AR, Burdette JH, et al. Migraine associated cerebral hyperperfusion with arterial spin-labeled MR imaging. AJNR Am J Neuroradiol 2008;29(8):1494–1497.
25. Yonas H, Pindzola RR, Meltzer CC, Sasser H. Qualitative versus quantitative assessment of cerebrovascular reserves. Neurosurgery 1998;42(4):1005–1010.
26. Newbould RD, Skare ST, Jochimsen TH, et al. Perfusion mapping with multiecho multishot parallel imaging EPI. Magn Reson Med 2007;58(1):70–81.
27. Wu O, Ostergaard L, Weisskoff RM, Benner T, Rosen BR, Sorensen AG. Tracer arrival timing-insensitive technique for estimating flow in MR perfusion-weighted imaging using singular value decomposition with a block-circulant deconvolution matrix. Magn Reson Med 2003;50(1):164–174.
28. Dai W, Garcia D, de Bazelaire C, Alsop DC. Continuous flow driven inversion for arterial spin labeling using pulsed radiofrequency and gradient fields. Magn Reson Med 2008; 60(6):1488–1497.
29. Macintosh BJ, Pattinson KT, Gallichan D, et al. Measuring the effects of remifentanil on cerebral blood flow and arterial arrival time using 3D GRASE MRI with pulsed arte-

rial spin labelling. J Cereb Blood Flow Metab 2008;28(8):1514–1522.

30. Olivot JM, Mlynash M, Zaharchuk G, et al. Perfusion-magnetic resonance imaging Tmax and mean transit time correlate with stable xenon computed tomography cerebral blood flow in stroke patients. Neurology 2009; 72(13):1140–1145.

31. Hendrikse J, van Osch MJ, Rutgers DR, et al. Internal carotid artery occlusion assessed at pulsed arterial spin-labeling perfusion MR imaging at multiple delay times. Radiology 2004;233(3):899–904.

32. Petersen ET, Lim T, Golay X. Model-free arterial spin labeling quantification approach for perfusion MRI. Magn Reson Med 2006; 55(2):219–232.

33. Alsop DC, Detre JA. Reduced transit time sensitivity in noninvasive magnetic resonance imaging of human cerebral blood flow. J Cereb Blood Flow Metab 1996;16(6): 1236–1249.

34. Campbell AM, Beaulieu C. Pulsed arterial spin labeling parameter optimization for an elderly population. J Magn Reson Imaging 2006;23(3):398–403.

35. Xie J, Gallichan D, Gunn RN, Jezzard P. Optimal design of pulsed arterial spin labeling MRI experiments. Magn Reson Med 2008;59(4):826–834.

36. Ye FQ, Mattay VS, Jezzard P, Frank JA, Weinberger DR, McLaughlin AC. Correction for vascular artifacts in cerebral blood flow values measured by using arterial spin tagging techniques. Magn Reson Med 1997; 37(2):226–235.

37. Wang J, Alsop DC, Song HK, et al. Arterial transit time imaging with flow encoding arterial spin tagging (FEAST). Magn Reson Med 2003;50(3):599–607.

38. Garcia DM, Duhamel G, Alsop DC. Efficiency of inversion pulses for background suppressed arterial spin labeling. Magn Reson Med 2005;54(2):366–372.

39. Alsop DC, Detre JA. Background suppressed 3D RARE arterial perfusion MRI [abstr]. In: Proceedings of the Seventh Meeting of the International Society for Magnetic Resonance in Medicine. Berkeley, Calif: International Society for Magnetic Resonance in Medicine, 1999; 22.

40. Fernandez-Seara MA, Edlow BL, Hoang A, Wang J, Feinberg DA, Detre JA. Minimizing acquisition time of arterial spin labeling at 3T. Magn Reson Med 2008;59(6):1467–1471.